# Durable Icephobic Coating for Stainless Steel

Ludmila B. Boinovich,[†,]* Alexandre M. Emelyanenko,[†] Vladimir K. Ivanov,[‡] and Andrei S. Pashinin[†]

[†]A.N. Frumkin Institute of Physical Chemistry and Electrochemistry, Leninsky prospect 31 bld. 4, 119071 Moscow, Russia
[‡]N.S. Kurnakov Institute of General and Inorganic Chemistry, Leninsky prospect 31, 119071 Moscow, Russia

Ⓢ Supporting Information

**ABSTRACT:** In this work, we present a modification of a stainless steel surface to impart superhydrophobic properties to it that are robust with respect to mechanical stresses associated with cyclic icing/deicing treatment, as well as to long-term contact with aqueous media and high humidity. The durability of the superhydrophobic state is ensured by the texture with multimodal roughness stable against mechanical stresses and a 2D polymer network of fluorooxysilane chemically bound to the texture elements. The designed superhydrophobic coating is characterized by contact angles exceeding 155° and a maximum rolling angle of 42° after 100 icing/deicing cycles.
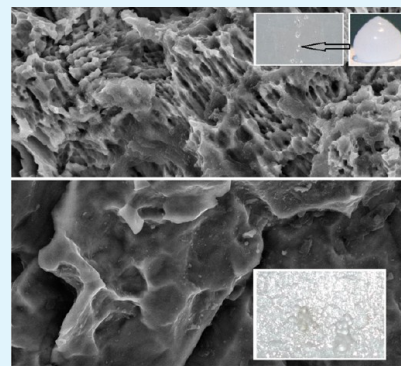


**KEYWORDS:** superhydrophobic surfaces, surface modification, functional coatings, durability, icephobicity

## ■ INTRODUCTION

Preventing ice adhesion and accumulation on surfaces has important applications in aviation, building construction, energy transmission, and conversion devices. For example, in aviation, ice accretions during flights alter the effective shape of the aircraft, modify the aerodynamic forces and moments caused by the air flow over iced components, and lead to the breakdown of gauging and control equipment. This affects the reliability of flights and may cause not only damage to the aircraft, but also loss of life, motivating researchers and engineers to develop new methods to mitigate the problem.

The application of aircraft deicing fluids on parked aircraft has proven effective in keeping air travel safe in icing conditions;[1] however, it is a high cost process and has an environmental impact. Moreover, these glycol-based liquids are harmful to helicopter components. Infrared or electric heating of aircraft wings or gauging and control equipment of aircraft and helicopters during flight reduces the icing problem; however, it does not always give the desired result.[2] Thus, the development of passive icephobic coatings is highly desirable.

Superhydrophobicity has been proposed as a leading passive anti-icing strategy due to several advantages of the super-hydrophobic state of a surface. Among other things, the main important attractive features of superhydrophobic surfaces are water repellency and low adhesion of liquid drops to these surfaces, resulting in removal of the drops from the surface before the water freezes.[3] The delay in freezing and heat transfer of liquid drops deposited onto a superhydrophobic surface are particularly advantageous for aviation applications to avoid icing while crossing atmospheric layers with high water content.[4] Finally, the low adhesion of ice, frost, and snow to

superhydrophobic surfaces (see, for example, refs 4 and 5) facilitates ice deposits removal under external load when they exceed some critical size.

An analysis of different mechanisms of superhydrophobic surface icephobicity was given in our recent paper.[4] It was shown there that all of the above-mentioned icephobicity mechanisms are based on a fact that the coating is wetted by both solid and liquid aqueous phase in a heterogeneous wetting regime. In this wetting regime, the aqueous medium only contacts the material at the surface of the protrusion peaks, while air is trapped inside the grooves of the surface relief. The effective contact angle is described by the Cassie−Baxter equation,[6] with the area of real contact between the liquid and the material characterized by the fraction of the wetted area, which is generally considerably less than 10%.

It should be noted that the question of whether super-hydrophobic surfaces always behave as anti-icing has been actively discussed in the recent literature (see, for example, refs 5 and 7−10). This very interesting and important issue was considered in our previous paper;[4] therefore, we will not dwell on this point here.

Another important issue pointed out in the literature[9−15] is that some superhydrophobic coatings show a lack of robustness to mechanical stresses, hydrolysis, and high humidity. Hydrolysis of fluorooxysilane components of coatings on long-term contact with aqueous media leads to degradation of hydrophobicity because of increasing surface energy. High humidity associated with vapor oversaturation causes vapor

condensation/desublimation into the coating grooves and a transition to the homogeneous (Wenzel) wetting regime. The mechanical stresses arising during ice detachment or icing/deicing cycles may result in deterioration of superhydrophobicity (anti-icing properties) because of gradual breaking of the surface asperities.

It was established that the fracture stress that occurs in capillary-porous systems under freezing depends on the relationship between the rate of ice formation and relaxability of excess local pressures emerging during icing. According to ref 16, these pressures vary in the range from $5 \times 10^4$ to $2 \times 10^8$ Pa.

Several approaches have been proposed to improve the resistance of superhydrophobic coatings to moderate shear stresses[17] and mechanical abrasion.[18] In this work, we present a treatment for a stainless steel surface leading to a superhydrophobic state with extreme robustness against long-term contact with aqueous media, high humidity, and cyclic icing/deicing impact. This treatment will be applicable for gauging and control equipment of aircraft and helicopters to improve air transportation safety. The main point addressed in this study was an analysis of the resistance of superhydrophobic coatings to hydrolysis, high humidity, and mechanical stresses caused by icing/deicing processes. Thus, we tried to answer the following questions: (1) Is the method used for texturing the steel surface resistant to the stresses acting on the sample surface in contact with water during water crystallization? As discussed in the literature,[9,13,19] this problem is of primary importance for industrial anti-icing application of superhydrophobic coatings. (2) Is the hydrophobic agent used in our work stable against hydrolysis on prolonged contact of the coating with water? (3) Does the coating degrade on prolonged contact with water?

## ■ MATERIALS AND METHODS

In this paper, we have studied superhydrophobic coatings formed on the surface of 12X18H10T stainless steel (an analog of 321H AISI). The morphology and elemental composition of a surface typical of an as-rolled sample of this type of steel is presented in the Supporting Information Figure S1 and Table S1.

The design of the coating included two stages. Chemical etching was performed at the first stage. Samples of stainless steel were immersed in 50 vol. % aqueous solution of $FeCl_3$ for 20 (sample 1), 40 (sample 2), or 60 min (sample 3). After exposition in etching solution, the samples were rinsed with distilled water until neutral pH of the washing solution was reached, then treated three times in an ultrasonic bath in distilled water for 5 min, dried with ash-free filter paper, and desiccated in an oven at 120 °C for 30 min. It is worth noting that the application of chemical etching methods to impart multimodal roughness to the metal surface has been shown in the literature (see, for example, refs 20 and 21). The second step consisted in depositing nanoparticles from a wetting film of dispersion, containing silica nanoparticles, the hydrophobic agent metoxy-{3-[(2,2,3,3,4,4,5,5,6,6,7,7,8,8,8-pentadecafluorooctyl)oxy]propyl}-silane, and dehydrated decane as a dispersion medium. The deposition method for these coatings was described in detail earlier[14] and leads to the creation of a multimodal structure formed by separate nanoparticles and their microscale aggregates.

Characterization of the wettability of the coating was based on contact and rolling angle measurements. We used the method of digital video image processing of sessile droplets. The homemade experimental setup for recording optical images of sessile droplets and software for subsequent determination of droplet parameters using the Laplace curve fitting routine were described earlier.[22,23] A Pixelink PL-B686MU monochrome digital camera with spatial resolution 1280 × 1024, color resolution 256 gray levels and time resolution 25 frames per second was used to capture the droplet images. The measured

initial contact angles correspond to advancing contact angles, as follows from the behavior of the contact diameter. To characterize the wetting of different coatings, initial contact angles for the 10−15 μL droplets were measured on five different surface locations for each sample, with the average angle for ten consecutive images of the droplet being defined for each place. The reproducibility of determining the contact angle defined as the root-mean-square deviation of angles for ten consecutive images of the droplet was better than 0.1°.

We have studied the stability of the superhydrophobic state of the coating both on long-term contact with water under saturated vapor pressure and in the cyclic icing/deicing procedure. The stability of the coating on long-term contact with water was studied by monitoring the evolution of the water contact angle, base diameter of the water droplet and liquid surface tension as functions of time. To make these measurements, a tested sample with a drop of testing liquid was placed inside the experimental chamber with 100% humidity atmosphere. The details of the experimental setup are given in ref 14. The simultaneous long-term measurements of contact angle, droplet base diameter, and liquid/vapor surface tension at very low drop evaporation rate made it possible to detect the deterioration of the contact angle resulting from the interaction of the coating with water and superhydrophobic state degradation.[12]

To measure the rolling angle, 10−15 μL droplets were deposited onto the surface. After the initial droplet shape was equilibrated, manipulation with an angular positioner allowed us to change the sample surface tilt in a controllable manner and detect the rolling angle by averaging over 5 different droplets on the same substrate.

The robustness of coating against mechanical stresses during icing was studied in the following cyclic icing/deicing procedure. The samples were placed in a container filled with distilled water and subjected to periodic variation of the temperature in a Binder MK53 Environmental Chamber. Each cycle included cooling to $T = −40$ °C over 30 min and exposition at that temperature for the next 30 min. Crystallization of the water in the container was checked up through the observation window. Then the temperature in the chamber was steadily raised to $T = +30$ °C over 30 min, and the samples were kept at that temperature for 30 min. After the desired number of icing/deicing cycles was repeated, the sample was taken from the container and dried with ash-free filter paper. The contact and rolling angles were measured immediately, then after drying in the laboratory air (temperature 21−23 °C, relative humidity 60−80%) for 2 and 16 h, and again after heat treatment in the oven at 140 °C for 2 h. The degradation of the coating in the icing/deicing cycles described above was assessed from the variation of water contact and rolling angles, on an analysis of surface SEM images, and on the EDX measurements of the elemental composition of the coatings.

In addition, a tape peeling test was performed to assess the mechanical stability of the coating with respect to silica particle detachment. For this purspose, ScotchA-810 adhesive tape was pressed against the coating with a pressure 130 kPa and then peeled off.

The second mechanical test was related to an analysis of coating resistance to cavitation erosion. A sample with the superhydrophobic coating was immersed in an ultrasonic bath with ultrasonic generator frequency 35 kHz and power 55 W for 10 min. After the sample was dried in the oven at 120 °C for 30 min and air cooled to room temperature, the contact and rolling angles were measured. For all the samples studied, it was found that the contact and rolling angles before and after both tape peeling and cavitation erosion tests coincided within the confidence interval of experimental data.

The microstructure of the samples was studied using a Carl Zeiss NVision 40 scanning electron microscope. Micrographs were taken at 1 and 15 kV acceleration voltages using secondary (InLens, SE2) and backscattered (ESB) electron detectors; the magnification range was from ×700 to ×350 000. Topographic and compositional information about the studied surfaces was extracted by comparing the images obtained with secondary and backscattered electrons. Energy-dispersive X-ray (EDX) analysis was performed using a built-in Oxford Instruments X-MAX analyzer equipped with an 80 mm²

**Table 1. Variation of Contact (CA) and Rolling (RA) Angles on Different Samples in the Cyclic Icing/Deicing Procedure**

| number of icing/deicing cycles | Sample 1 | | Sample 2 | | Sample 3 | |
|---|---|---|---|---|---|---|
| | CA, deg | RA, deg | CA, deg | RA, deg | CA, deg | RA, deg |
| 0 | 168.7 ± 4.8 | 9.6 ± 2.9 | 169.7 ± 4.2 | 7.6 ± 3.3 | 166.1 ± 2.5 | 10.6 ± 3.9 |
| 5 | 162.3 ± 2.3 | 12.2 ± 4.3 | 163.1 ± 4.9 | 10.2 ± 2.2 | 165.9 ± 2.5 | 15.2 ± 2.6 |
| 50 | 160.3 ± 1.0 | 11.0 ± 4.3 | 161.1 ± 3.7 | 17.8 ± 5.0 | 156.0 ± 1.7 | 31.8 ± 15.2 |
| 100 | 160.7 ± 2.1 | 12.7 ± 4.8 | 161.6 ± 2.4 | 17.1 ± 6.0 | 155.4 ± 3.8 | 42.3 ± 10.0 |

detector at 20 kV acceleration voltage. EDX data for each sample were collected from five different spots of ~10−70 $\mu m^2$ each.

## ■ RESULTS AND DISCUSSION

The three types of superhydrophobic samples differed from each other in chemical etching time, as described above in the experimental section. The initial advancing angles, as well as rolling angles for all samples with coatings, are presented in the first row of Table 1. As follows from the experimental data, all samples demonstrate the superhydrophobic state with contact angle >150° and low rolling angles.

The stability of superhydrophobicity was analyzed by monitoring the evolution of the contact angle and liquid surface tension of a droplet on the samples. This analysis is demonstrated for sample 3, where the contact angles decreased by only a few degrees after 5 days of contact with water, as shown in Figure 1. The surface tension of the liquid drop is
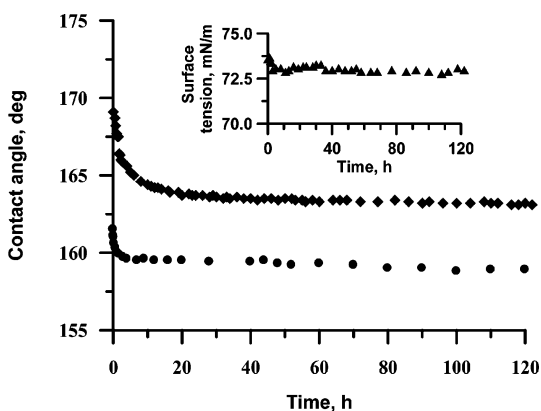


**Figure 1.** Evolution of the contact angle of the water droplet on sample 3 in a saturated vapor environment before (diamonds) and after (circles) 100 icing/deicing cycles. The inset shows the evolution of surface tension of the drop deposited onto the sample.

almost constant, indicating that the hydrophobic molecules are not desorbed from the coating even on prolonged contact with water. The surface remained in the superhydrophobic state with a final contact angle of ~163°. Furthermore, in spite of this long exposure time at saturated vapor conditions, the coating preserved low wetting hysteresis and water droplets continued to roll off the samples at low sample tilts of <20°.

Analysis of the morphology and composition of all coatings indicates that nanoparticles coated with a hydrophobic agent shell decorate the surface texture of stainless steel with a dense layer. Aggregates of nanoparticles are also present on the surface of coating. This is demonstrated in Table 2 by the normalized elemental composition evaluated by energy-dispersive X-ray (EDX) analysis. The spots on the surface of sample 3, from which the EDX data of Table 2 were collected, are shown in Figure 2.
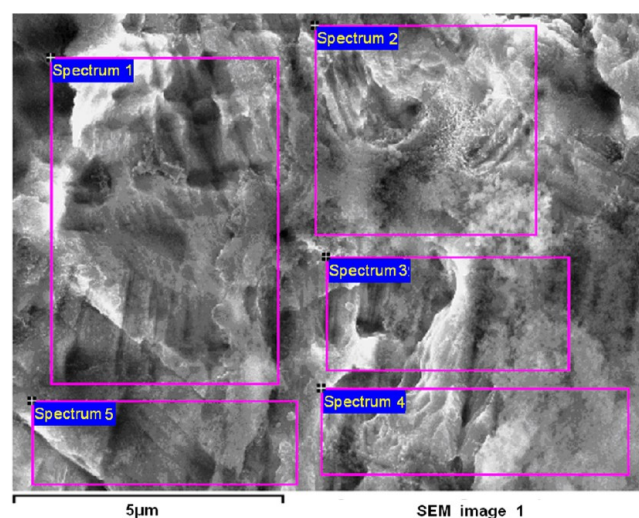


**Figure 2.** SEM image of the surface of the superhydrophobic coating on stainless steel (sample 3) indicating the spots at which the EDX spectra reported in Table 2 were collected.

The increased amount of Si indicates enrichment of the surface with aggregates of $SiO_2$ nanoparticles. At the same time, fluorooxysilane molecules are present in the coating both in the adsorption layer on the steel surface and on the surface of the nanoparticles. It should be emphasized that the stage of chemical treatment of steel affects both the morphology of the surface and its chemical composition (cf. also chemical compositions of samples before and after the chemical etching presented in the Supporting Information Table S1). As follows from the data of Table 2 and Table S1, the surface layer of steel loses titanium to a greater extent, iron and nickel to a lesser extent and is enriched with chromium. This change in the

**Table 2. Normalized Elemental Composition (at. %) of the Coating on Sample 3**

| | C | O | F | Si | Ti | Cr | Mn | Fe | Ni |
|---|---|---|---|---|---|---|---|---|---|
| spectrum 1 | 20.9 | 7.0 | 8.4 | 2.3 | 0.2 | 12.4 | 1.1 | 42.9 | 5.0 |
| spectrum 2 | 24.2 | 10.9 | 8.8 | 4.0 | 0.2 | 10.4 | 1.0 | 36.3 | 4.3 |
| spectrum 3 | 22.4 | 10.7 | 7.8 | 3.6 | 0.2 | 10.9 | 1.0 | 38.7 | 4.6 |
| spectrum 4 | 28.0 | 12.0 | 12.9 | 4.4 | 0.1 | 8.6 | 0.8 | 29.7 | 3.6 |
| spectrum 5 | 24.9 | 7.4 | 8.1 | 2.8 | 0.2 | 11.2 | 1.0 | 39.7 | 4.7 |

surface layer composition will promote an increase in corrosion resistivity and hardness of the surface layer. In our opinion, the noticeable increase in carbon content in the surface layer is related to capillary filling of nanopores (formed during chemical etching) by decane at the dispersion deposition stage. As a result of the low vapor pressure of the hydrocarbon liquid and nanosize of the pores, the pores remain filled with decane even after high temperature (at 140 °C) and vacuum treatment of the coatings. The presence of this hydrocarbon liquid inside the pores should prevent partial penetration of water into the pores and decrease deformation stresses during phase transition. As a result, higher mechanical stability of the coating against icing/deicing treatment is expected.

We have tested the ability of samples with coatings to reduce the accumulation of snow and ice. Figure 3 shows the



**Figure 3.** Outdoor test of comparative behavior of sample 3 with a superhydrophobic coating (top) and untreated stainless steel (bottom) in heavy snowfall at −3 °C, relative humidity 99%, and wind velocity 2 m s$^{-1}$.

comparative behavior of sample 3 with a superhydrophobic coating (top) and untreated stainless steel (bottom) in heavy snowfall at −3 °C. The significant difference in the samples is due to the fact that wet heavy snow falling onto crude steel remains fixed on the surface, followed by accumulation. At the same time, the low adhesion of snow to the superhydrophobic

surface contributes to its spontaneous removal under wind load and/or vibration of the stand. Comparative analysis of the behavior of the samples in freezing rain at −6 °C and humidity 97% showed that a continuous crust of thick, glassy ice was formed on the untreated surface in a few minutes. On the sample with the superhydrophobic coating, separate frozen droplets located on wetting defects were formed after prolonged exposure (about 25−30 min) to freezing rain. The contact angles formed by iced drops on superhydrophobic coatings varied in the range of 154−160°, and the drops demonstrated delayed freezing in comparison to freezing time for drops of supercooled water atop the untreated steel surface.

To examine the robustness of surface morphology and composition against mechanical stresses, we subjected all samples to cyclic icing/deicing treatment. The contact and rolling angles measured after a certain number of icing/deicing cycles and drying in the laboratory air for 2 h are presented in Table 1. From the data of Table 1, it follows that all samples show some degradation associated with insignificant deterioration of the contact angle and an increase in rolling angle. However, the analysis of the evolution of water contact angle, base diameter of the water droplet (not shown) and liquid surface tension as functions of time on prolonged contact with water (Figure 1) indicates that all samples still exhibit the superhydrophobic state. This superhydrophobic state is characteristic of the samples after 100 cycles of deformation stresses and more than 200 h of contact with aqueous media in wide range of variable temperatures. Monitoring of surface morphology and composition (Figure 4) indicates high robustness of both characteristics against the above-mentioned tests. SEM images of the surfaces of sample 1 before and after 100 icing/deicing cycles are shown in Figure 4. Similar images for sample 3 are presented in the Supporting Information (Figure S2). As follows from the analysis of the composition and morphology, the main difference in the surface texture and composition of the samples is related to a decrease in the number of nanoparticle aggregates. This is clearly illustrated by a comparison of two images of the same spot on the sample after 100 icing/deicing cycles obtained by using SE2 (Figure 4b) and ESB (Figure 4c) electron detectors. At the same time, a layer of nanoparticles decorating the texture elements remains on the surface (Figure 5). To test the stability of the superhydrophobic state of sample 3 after 100 icing/deicing cycles, the evolution of contact angle on long-term contact with water in saturated vapor environment was monitored (Figure 1, circles). The stationary state with contact angle of about 160°
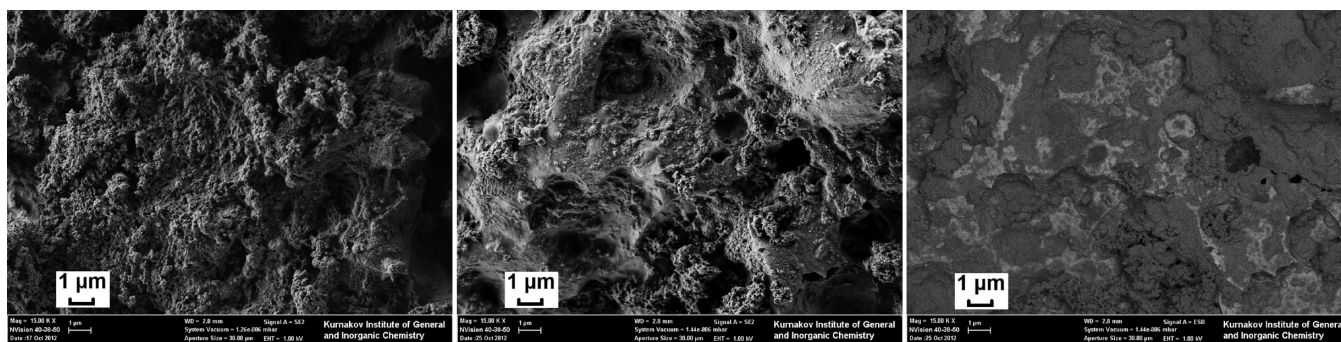


**Figure 4.** SEM images of sample 1 of stainless steel with the superhydrophobic coating before icing/deicing test (a) and after 100 icing/deicing cycles (b, c). Images a and b were registered using an SE2 secondary electron detector, and image c was registered using ESB backscattered electron detector.
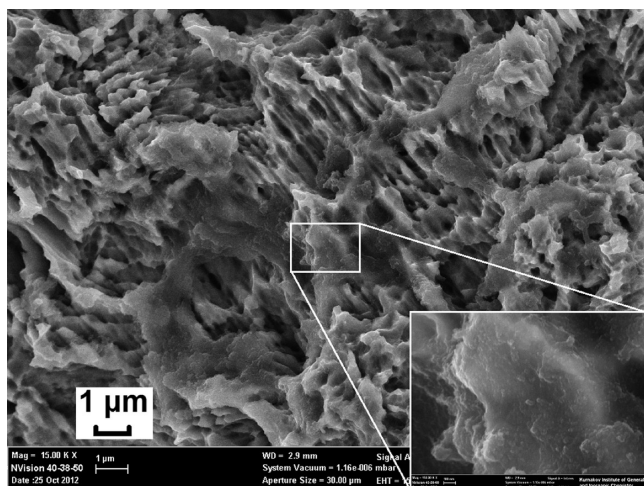
**Figure 5.** SEM image of sample 2 of stainless steel with the superhydrophobic coating after 100 icing/deicing cycles. The inset shows details of the coating structure.

established in a few hours indicates the durability of surface superhydrophobicity.

To learn more about the influence of the cyclic icing/deicing procedure on the state of the coating, we studied the contact and rolling angles on sample 3 as a function of the number of cycles (Figure 6). The angles were measured just after
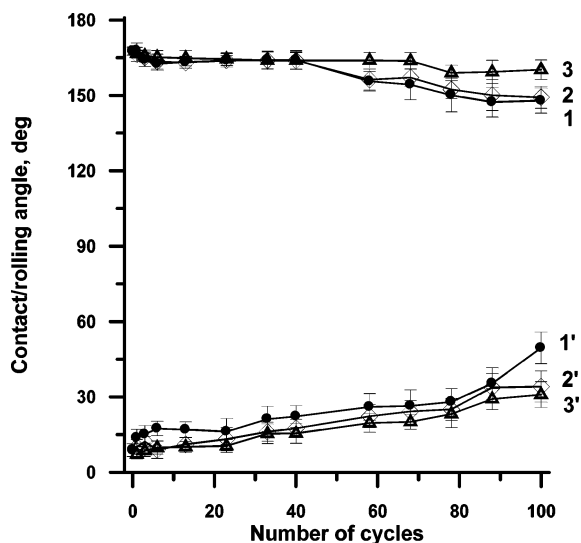


**Figure 6.** Dependence of contact (lines 1−3) and rolling (lines 1′−3′) angles on the number of icing/deicing cycles. One and 1′ correspond to angles measured just after removing the sample from the aqueous phase, 2 and 2′ to those after drying in the laboratory air for 2 h, and 3 and 3′ to angles after heat treatment in the oven at 140 °C for 2 h.

removing the sample from the aqueous phase, then after drying in the laboratory air for 2 h, and after heat treatment in the oven at 140 °C for 2 h. The change in contact and rolling angles during air and oven drying after long-term contact with the aqueous phase indicates two important properties of the designed coatings.

On one hand, there is an interaction between the hydrophobic agent and the aqueous medium, leading to hydration of individual fragments of the hydrophobic agent molecule (as we have shown earlier,[14] this is the hydration of

oxygen atoms in the molecule and hydration of terminal hydroxyl groups).

On the other hand, the hydrolysis of Si−O−Si and Si−O−Fe bonds leads to the formation of silanol groups, which are intensively hydrated by water, and to the formation of hydroxyl groups bound to the surface atoms of the metal. This results in the deterioration of the contact angle. The substantial increase in the contact angle and decrease in the rolling angle after heat treatment lead us to conclude that the basic process here is apparently the hydrolysis of Si−O−Si bonds. The partial restoration of contact and rolling angles for the sample subjected to 100 icing/deicing cycles, then dried for 168 h and heat treated at $T = 140$ °C, is evidently related to the chemical reaction

$$-\rangle Si-O-H + H-O-Si\langle-$$
$$\leftrightarrow -\rangle Si-O-Si\langle- + H_2O$$
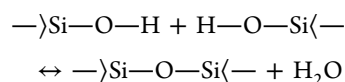
At high temperatures, equilibrium in this reaction is shifted toward the formation of siloxane bonds.

At the same time, it should be noted that an increase in the contact angle and a decrease in the rolling angle for the sample dried in air for a long time after immersion in water (Figure 7)
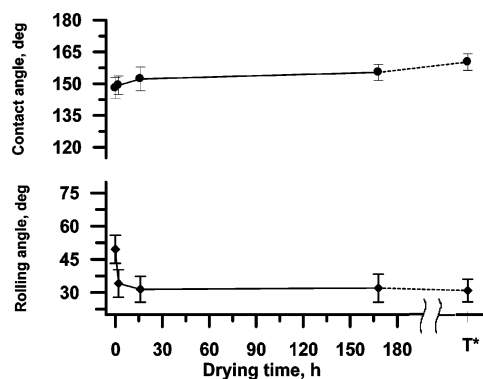


**Figure 7.** Dependence of initial contact angles and rolling angles for sample 3 on air drying time after 100 icing/deicing cycles. The abscissa point marked $T^*$ corresponds to measurements after heat treatment at $T = 140$ °C for 2 h.

indicates reversible hydration of individual fragments of the hydrophobic agent molecules. Therefore, we can speak of the manifestation of a self-healing, highly hydrophobic (superhydrophobic) state, which is crucial for long-term use of superhydrophobic coatings.

## ■ CONCLUSIONS

In this study, we have described a treatment for stainless steel that imparts superhydrophobic surface properties. Analysis of the resistance of superhydrophobic coatings to mechanical stresses, hydrolysis and high humidity was the main point addressed in this study. From the experimental data of scanning electron microscopy, dynamics of wetting and evolution of wetting characteristics during drying presented above, we conclude that some changes in surface morphology and hydrolysis of a small proportion of siloxane bonds takes place in the first few cycles of icing/deicing tests. However, after 100 icing/deicing cycles, accompanied by mechanical stresses and long-term contact with water, and after long-term contact with saturated vapor, the coatings still demonstrate multimodal roughness, low surface energy and stability of the super-

2553

dx.doi.org/10.1021/am3031272 | ACS Appl. Mater. Interfaces 2013, 5, 2549−2554

hydrophobic state. Thus the long-term robustness of super-hydrophobic properties under cyclic temperature variation and stresses characteristic of phase transition, as well as partial self-healing of wetting characteristics during air drying and heat treatment, allows us to consider these coatings designed for stainless steel as anti-icing coatings.

## ■ ASSOCIATED CONTENT

### Ⓢ Supporting Information

The SEM image of the surface of as-rolled stainless steel sample, normalized elemental composition of stainless steel samples before and after chemical etching, and the SEM images of sample 3 of stainless steel with a superhydrophobic coating before icing/deicing tests and after 100 icing/deicing cycles. This material is available free of charge via the Internet at http://pubs.acs.org.

## ■ AUTHOR INFORMATION

### Corresponding Author

*E-mail: boinovich@mail.ru.

### Notes

The authors declare no competing financial interest.

## ■ ACKNOWLEDGMENTS

## ■ REFERENCES

(1) *Preliminary Data Summary Airport Deicing Operations (revised)*, EPA-821-R-00-016; U.S. Environmental Protection Agency: Washington, DC, 2000.

(2) Koenig, G. G.; Ryerson, C. C. *Cold Reg. Sci. Technol.* **2011**, *65*, 79−87.

(3) Antonini, C.; Innocenti, M.; Horn, T.; Marengo, M.; Amirfazli, A. *Cold Reg. Sci. Technol.* **2011**, *67*, 58−67.

(4) Boinovich, L. B.; Emelyanenko, A. M. *Mendeleev Commun.* **2013**, *23*, 3−10.

(5) Dodiuk, H.; Kenig, S.; Dotan, A. *J. Adhes. Sci. Technol.* **2012**, *26*, 701−714.

(6) Cassie, A.; Baxter, S. *Trans. Faraday Soc.* **1944**, *40*, 546−551.

(7) Nosonovsky, M.; Hejazi, V. *ACS Nano* **2012**, *6*, 8488−8491.

(8) Meuler, A. J.; McKinley, G. H.; Cohen, R. E. *ACS Nano* **2010**, *4*, 7048−7052.

(9) Kulinich, S. A.; Farhadi, S.; Nose, K.; Du, X. W. *Langmuir* **2011**, *27*, 25−29.

(10) Jung, S.; Dorrestijn, M.; Raps, D.; Das, A.; Megaridis, C. M.; Poulikakos, D. *Langmuir* **2011**, *27*, 3059−3066.

(11) Varanasi, K. K.; Deng, T.; Smith, J. D.; Hsu, M.; Bhate, N. *Appl. Phys. Lett.* **2010**, *97*, 234102.

(12) Boinovich, L.; Emelyanenko, A. *Adv. Colloid Interface Sci.* **2012**, *179*, 133−141.

(13) Farhadi, S.; Farzaneh, M.; Kulinich, S. A. *Appl. Surf. Sci.* **2011**, *257*, 6264−6269.

(14) Boinovich, L. B.; Emelyanenko, A. M.; Pashinin, A. S. *ACS Appl. Mater. Interfaces* **2010**, *2*, 1754−1758.

(15) Verho, T.; Bower, C.; Andrew, P.; Franssila, S.; Ikkala, O.; Ras, R. H. A. *Adv. Mater.* **2011**, *23*, 673−678.

(16) Zaleski, A.; Florensky, B. V. *Proc. Inst. Geol. Sci. Acad. Sci. USSR* **1952**, *146*(42), 39−50 (in Russian).

(17) Ke, Q.; Fu, W.; Jin, H.; Zhang, L.; Tang, T.; Zhang, J. *Surf. Coat. Technol.* **2011**, *205*, 4910−4914.

(18) Xiu, Y.; Liu, Y.; Hess, D. W.; Wong, C. P. *Nanotechnology* **2010**, *21*, 155705.

(19) Menini, R.; Ghalmi, Z.; Farzaneh, M. *Cold Reg. Sci. Technol.* **2011**, *65*, 65−69.

(20) Li, L.; Breedveld, V.; Hess, D. W. *ACS Appl. Mater. Interfaces* **2012**, *4*, 4549−4556.

(21) Qian, B. T.; Shen, Z. Q. *Langmuir* **2005**, *21*, 9007−9009.

(22) Emelyanenko, A. M.; Boinovich, L. B. *Instrum. Exp. Tech.* **2002**, *45*, 44−49.

(23) Emel'yanenko, A. M.; Boinovich, L. B. *Colloid J.* **2001**, *63*, 159−172.